Study of Entropy Generation in Secondary Flows in the T106A Low Pressure Axial Turbine Cascade

Vanamala Uma Maheshwar[1](✉) and Apalla Aditya Shiva[2]

[1] Department of Mechanical Engineering, Osmania University, Hyderabad 500007, India
mahesh.v@uceou.edu
[2] Mechademy Engineering Solutions Pvt. Ltd, New Delhi 110048, India

Abstract. The T106 axial turbine series is used extensively by major engine manufacturers, because of its ability to give the best performance at low pressure conditions. However, it has high secondary flow development. The present work aims at understanding the effect of high gas velocities and high temperatures on secondary flows in the T106A Low Pressure Turbine cascade for both smooth and rough blade surfaces. CFD analysis has been conducted using ANSYS CFX v19.1 using the k – ε model for turbulence and the total energy model for overall analysis, for five velocities and a fixed high temperature which was imposed using the total temperature equation. It was observed that there was no variation in the overall pressure profile for smooth and rough blade surfaces, and there was a large positive pressure coefficient. However, there was a high rate of entropy generation and turbulent kinetic energy production rate, accompanied by high heat transfer coefficients in the case of rough blade surface. For the case of the rough blade, as compared to the smoother blade, the boundary layer separation increased further affront towards the leading edge with increase in gas velocity and surface roughness along with increasing Turbulent Kinetic Energy (TKE) in both the cases.

Keywords: Axial turbine cascade · secondary flows · entropy generation · turbulent kinetic energy

1 Introduction

The Low-Pressure Turbine (LPT) is a robust machine working in a mixture of adverse environments and thus its design is rather tricky. Used in gas turbine (GT) engines, the LPT is a large machine with operating Mach numbers ranging from 0.4 – 0.7, thus constituting a transonic turbine stage. The latter stages of the LPT have very low densities of flue gases, allowing last stages to handle very high volumes, leading to a system of highly loaded blades delivering the largest fraction of the overall energy generated to the thrust fan, and thus these blades are sometimes referred to as high lift blades (Hurda, 2016) [1]. These cascades have high pitch to chord ratios –3 to 7, leading to an extremely unusual level of offset from each other. As a result of which, the flow turning angle is

© The Author(s) 2023
B. Raj et al. (Eds.): ICETE 2023, AER 223, pp. 1189–1196, 2023.
https://doi.org/10.2991/978-94-6463-252-1_119

very high in LPT cascades. Typically, the efficiency of the LPT ranges between 90% and 93%. Even with such magnificent numbers to speak of, the aerodynamics of the LPT is extremely critical and unsteady. The flow is inherently three dimensional due to the blade passage geometry with features such as twisting of the blade along the span, clearance between the blade tip and the shroud, film cooling holes, and end wall contouring. The passage flow is characterized by boundary layer (BL) effects, secondary flows generated by the passage pressure gradients, and vortical flow structures such as the leading edge (LE) horse-shoe vortices, tip-leakage flow vortices, and corner vortices. Mc Quilling (2007) [2] has elaborately discussed the two key flow impedances leading to unsteady nature of flows in an LPT passage – passage unsteadiness and low-Re effects. While the passage unsteadiness is a result of the wakes and secondary flows in the endwall regions of the passage, the low-Re effects manifest in the form of the flow's poor resistance to turbulent separation at the TE of the blade. This poor interaction of the flow leads to (a) reduced efficiency and (b) increased fuel consumption.

2 Literature Survey

A broad aspect of the losses in the flow path of the cascades has been shown in Fig. 1, as described by Zou et al. [3], which dictate that the maximum loss is dues to profile loss, which is basically an outcome of the secondary flow field in the LPT. The LPT's, possessing high aspect ratios, require shrouds and therefore, an estimation of the tip clearance losses is rather redundant.

Stieger and Hodson [4] conducted experimental investigations regarding the nature of dissipation of turbulent kinetic energy (TKE) in the downstream region. Turbulent stresses are produced when a wake, generated by the system designed, passes over a region of high spatial velocity gradient. Depending on the vectorial orientation of the wake and the gradients, the overall intensity is either enhanced or reduced. This turbulence is dissipated in the form of a bow – elongated compared to the inlet bow and stretched along the region passing from the midspan to the TE of the blade.

Cui et al. [5] performed numerical investigation into the secondary flows in the T106A cascade. The computational mesh was set for $0.4C_x$ upstream and $1.3C_x$ downstream. The mass–averaged total pressure loss coefficient and loss generation rate were measured. The following conclusions were made:

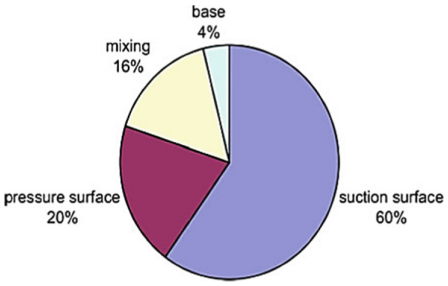

Fig. 1. Distribution of blade losses across the flow path (Zou, 2018) [3]

i. The turbulent BL and wake had a more prominent eddy and secondary flow system than the laminar BL.
ii. Upstream of the transition point, the loss generation rate was very high. However, downstream of it, the separation bubble was suppressed by the presence of the incoming wakes.
iii. The loss generation rate was slower in the far downstream regions than the mid span regions, due to the rapid mixing of the wakes.

Montis et al. (2010) [6] investigated the effect of surface roughness on the boundary layer characteristics of the cascade. Three roughness profiles represented in the form of surface roughness to chord ratio were taken. Profile loading, loss and boundary layer measurements were done for turbulence levels ranging from 3% to 6% from Reynolds numbers 5×10^4 to 7×10^5. The investigations revealed that there was absolutely no variation in the pressure profile as compared to that of a smooth blade. Winhart (2021) [7] observed that for a transonic airfoil, turbulent separation is further enhanced by Kelvin-Helmholtz instability downstream of the passage, augmenting wall heat transfer.

3 Test Case and Boundary Conditions

3.1 Grid Independence Study

The T106 series of cascade airfoils is one of the greatest achievements in the development of LPT airfoils which were a result of consistent research and development by Hoheisel et al. [8] in conjunction with renowned GT engine manufacturer Pratt & Whitney. The T104 – T106 family includes airfoils with both front and aft loading with values of the non – dimensional Zweifel coefficient, Z, of approximately 1.04–1.07. The test case has been described in Fig. 2.

Grid independence study was conducted on the test case per the conditions used by Garai et al. [9] for four mesh sizes from 0.0048 to 0.0052 m. The results of the grid independence study are shown in Fig. 3. Following this study, the mesh was set at 472,680 elements and 1,997,100 nodes, and the mesh size was set at 0.0048 m.

Dimension	Value
Chord (C)	198 mm
Axial Chord (C_x)	170 mm
Pitch (P)	158 mm
Span (H)	375 mm
Inlet flow angle (α_1)	37.7°
Exit flow angle (α_2)	63.2°
Blade Stagger (γ)	30.84°
Flow Coefficient (ϕ)	0.83

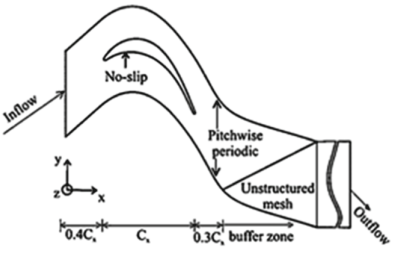

Fig. 2. (a) T106A Cascade Geometry, and (b) T106A Cascade used by Cui et al. [5]

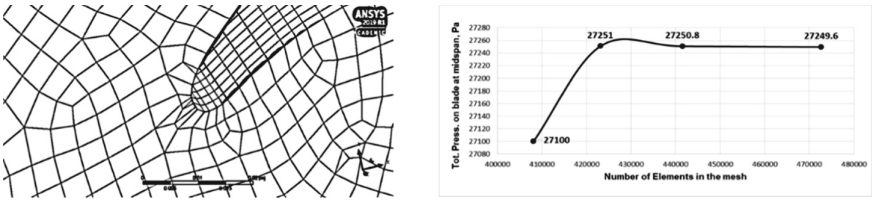

Fig. 3. (a) Mesh View of the Test Case, and (b) Results of Grid Independence Study

3.2 Boundary Conditions

The present work seeks to study the flow patterns and examine the nature of secondary flows in the T106A Low Pressure Turbine cascade in the high velocity range of 450 m/s–500 m/s flowing at high temperature at a cruising altitude of 10 km [10]. From the principles of atmospheric thermodynamics, we know that,

$$T_h = T_g - \lambda h \tag{1}$$

$$\left(\frac{p_h}{p_g}\right) = \left(\frac{T_h}{T_g}\right)\exp\left(\frac{g}{\lambda R}\right) \tag{2}$$

where λ is the atmospheric lapse rate = 65 K/1000 m = 0.0065 K/m, h is the height, g = 9.80665 m/s^2 and R is the gas constant for air = 287.05287 J/kg K. Thus, for the study, the inlet BC's are the fluid velocity and temperature (Table 1) while the exit BC is the ambient pressure, i.e., 26436.4 Pa.

The wall is set to no slip condition and the flow domain is set as symmetry BC. The residuals have been set at RMS levels 0.0001. The k – ε model is selected for turbulence and the fluid turbulence is set at 5%.

4 Results and Discussion

The value of Coefficient of pressure, C_p is estimated using Eq. (3), from $x/C_x = 0.4$ to 1.4. It is observed from Fig. 4. That the blade experience positive and higher loading on the aft, due to its geometry and also, there is no appreciable difference in pressure

Table 1. Test conditions under constant static temperature and varying surface roughness

S. No.	Velocity (v), m/s	Static Temperature (T), °C	Surface Roughness, μm
1	450	500	10
2	462		10
3	475		15
4	488		20
5	500		30

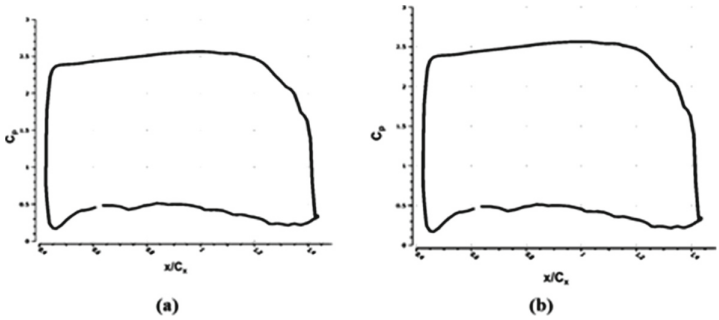

Fig. 4. Cp Plots for (a) Smooth Wall, and (b) Rough Wall at 10 μm surface roughness

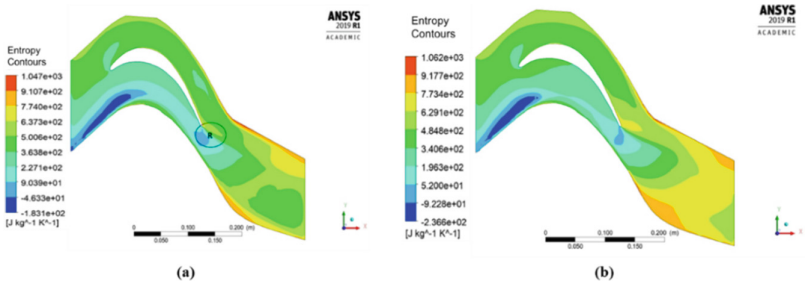

Fig. 5. Entropy Gen. for (a) Smooth Wall, and (b) Rough Wall at 10 μm surface at 450 m/s

distribution due to the effect of surface roughness, in accordance with Montis et al. [6].

$$C_p = \frac{\text{Pressure on the blade} - 26436.24}{0.5 \times \rho_{avg} \times v_{in,\,avg}{}^2} \tag{3}$$

4.1 Nature of Entropy Generation

The region marked R in Fig. 5 represents the zone of high recirculation and mixing, thus indicating varied and high levels of entropy generation in the flow passage. As the velocity increases along with surface roughness, the distribution of higher entropy generation around the endwalls on the suction side increased and tend to move forwards. Also, it is observed that as the surface roughness increases, the region of low entropy generation around the pressure side end wall diminishes. Figure 6 shows that the max. Entropy generation reduces slightly at 488 m/s before increasing.

4.2 Analysis of Turbulent Kinetic Energy (TKE) Contours

The production of turbulent KE indicates a flaring pattern at the trailing edge of the airfoil, with peak production very close to the endwall at the trailing edge as in Fig. 7 and 8. For both the cases, i.e., rough, and smooth walls, there is an established correlation

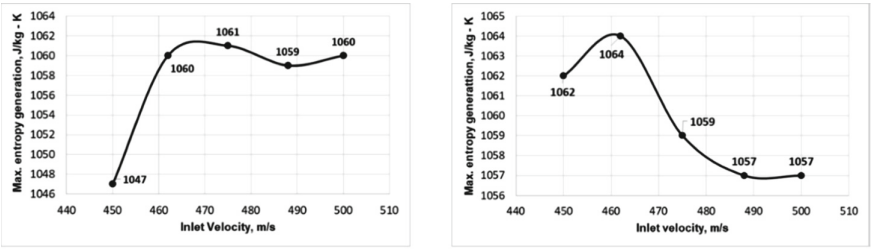

Fig. 6. Variation of Max. Entropy Generation Rate in the Cascade Vs Inlet Velocity for (a) Smooth Wall, and (b) Rough Wall

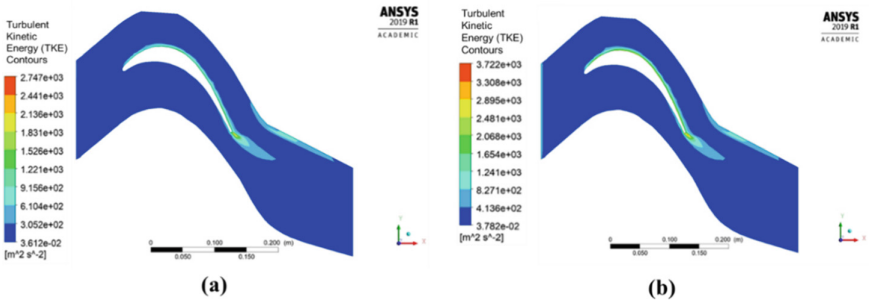

Fig. 7. TKE Contours for (a) Smooth Wall, and (b) Rough Wall at 30 μm roughness at 500 m/s

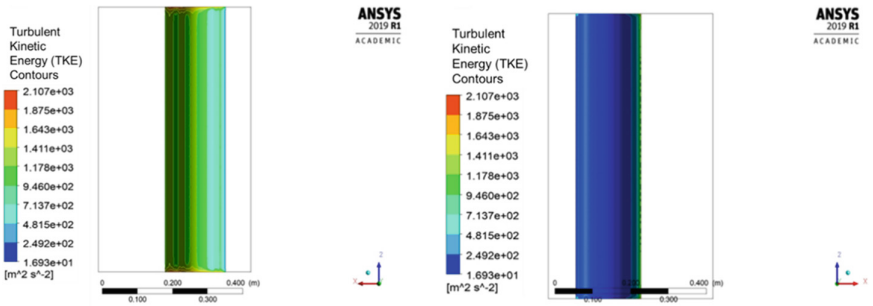

Fig. 8. TKE Contours for (a) Suction surface, and (b) Pressure surface

between the widening TKE flare and the reduction of low entropy generation regions, as the velocity and surface roughness are increased. This is attributed to the larger mixing of flows in the regions of higher energy fluxes. The incoming high energy flow undergoes rapid mixing and with the introduction of surface roughness, the TKE contours show a marked frontal movement with the thickness of TKE increasing around the theoretical length from where the secondary flows develop in the cascade i.e., roughly around 0.6 C_x as shown in Fig. 9 with max. TKE increasing with velocity.

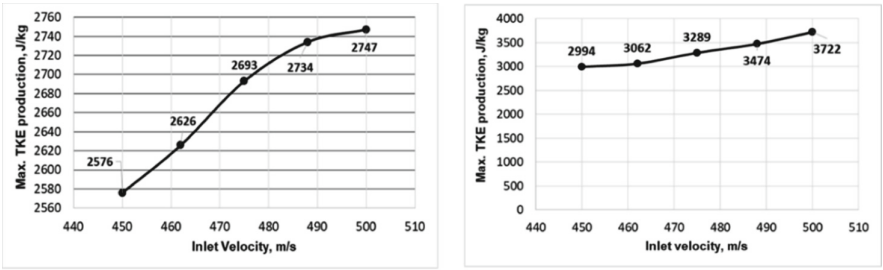

Fig. 9. Variation of Max. TKE Production in the Cascade Vs Inlet Velocity for (a) Smooth Wall, and, (b) Rough Wall

5 Conclusions

The present work involves the study of secondary flows in the T106A low pressure axial turbine cascade. CFD Analysis was conducted to study the effect of high velocity and temperature at an altitude of 10,000 m. First, analysis was done for smooth wall and then the wall surface roughness was changed for the same set of parameters. Results are presented in the form of pressure coefficient graphs along with the contours of entropy generated in the flow passage, Turbulent kinetic energy generated across the blade passage. Based on the results, the following conclusions are drawn:

5.1 Analysis of Pressure Profile

There was no difference caused to the pressure profile of the cascade on account of inclusion of surface roughness as input. However, the cascade experienced higher aft loading and thus, it developed positive pressure coefficients on both suction and pressure side.

5.2 Nature of Entropy Generation and Distribution

In both cases, the entropy contours were nearly the same. However, with the smooth wall, the maximum entropy generated first increased and then saturated, while for the rough wall, the peak entropy decreased marginally. This can be attributed to flow interactions with roughness of the surface resulting in entropy decrease. But, for the rough wall, regions of low entropy near the endwall regions on the pressure side of the blade thinned out sooner than expected as there was added mixing from the suction side to the pressure side on the trailing edge – endwall interface.

5.3 Analysis of Turbulent Kinetic Energy (TKE) Contours

For both the smooth and the rough wall, the TKE generation didn't exhibit the bowing effect and the maximum value of TKE increased continuously. This is attributed to higher flow velocities upstream, resulting in very high active mixing, smoothening out

any minor changes in TKE production. However, a TKE flare is developed near the trailing edge along with a boundary layer pattern, due to interaction of passage vortices on both sides of the blade. With increase in velocity, the TKE flare elongated and with increasing roughness, there was a widening of the TKE flare along with added roughness. Also, a significant level of TKE was generated on the suction side of the passage in the case of rough walls along with advanced boundary layer separation.

References

1. Hurda, L: Large eddy simulation of a turbulent flow around a low pressure turbine blade, University of West Bohemia (2016).
2. McQuilling, Mark W.: Design and Validation of a High-lift Low-pressure Turbine Blade, Wright State University (2007).
3. Zou Z., et al: Flow Mechanisms in Low-Pressure Turbines. In: Axial Turbine Aerodynamics for Aero-engine, pp 143–257, Springer, Singapore (January 2018).
4. Steiger, Rory D. and Hodson, H.P.: The Unsteady Development of a Turbulent Wake through a Downstream Low Pressure Turbine Blade Passage, Transactions of the ASME, Volume 127, pp 388–394 (April 2005).
5. J. Cui et al: Numerical investigation of secondary flows in a high-lift low pressure turbine, International Journal of Heat and Fluid Flow (2016).
6. Montis, Marco, et al: Effect of Surface Roughness on Loss Behaviour, Aerodynamic Loading and Boundary Layer Development of a Low Pressure Gas Turbine Airfoil, Proceedings of ASME Turbo Expo 2010: Power for Land, Sea and Air GT2010, UK (June 2010).
7. Winhart, B.: Large Eddy Simulation of a Modified T106 Low Pressure Turbine Stator under Periodic Wake Conditions, Ruhr-Universität Bochum, 2021.
8. Hoheisel, H, et al: Influence of Free Stream Turbulence and Blade Pressure Gradient on Boundary Layer and Loss Behavior of Turbine Cascades, Journal of Turbomachinery, Transactions of the ASME, Volume 109, pp. 210–219 (April 1987).
9. Garai, Anirban, et al: DNS of Flow in a Low-Pressure Turbine Cascade Using a Discontinuous Galerkin Spectral – Element Method, Proceedings of ASME Turbo Expo 2015: Turbine Technical Conference and Exposition GT2015, Canada (2015).
10. Fundamentals of Gas Turbine Engines by Commercial Aviation Safety Team., USA

Open Access This chapter is licensed under the terms of the Creative Commons Attribution-NonCommercial 4.0 International License (http://creativecommons.org/licenses/by-nc/4.0/), which permits any noncommercial use, sharing, adaptation, distribution and reproduction in any medium or format, as long as you give appropriate credit to the original author(s) and the source, provide a link to the Creative Commons license and indicate if changes were made.

The images or other third party material in this chapter are included in the chapter's Creative Commons license, unless indicated otherwise in a credit line to the material. If material is not included in the chapter's Creative Commons license and your intended use is not permitted by statutory regulation or exceeds the permitted use, you will need to obtain permission directly from the copyright holder.